

Corrected subdivision approximation of piecewise smooth functions

Sergio Amat,^{*} David Levin,[†] Juan Ruiz-Álvarez[‡]

Abstract

Subdivision schemes are useful mathematical tools for the generation of curves and surfaces. The linear approaches suffer from Gibbs oscillations when approximating functions with singularities. On the other hand, when we analyze the convergence of nonlinear subdivision schemes the regularity of the limit function is smaller than in the linear case. The goal of this paper is to introduce a corrected implementation of linear interpolatory subdivision schemes addressing both properties at the same time: regularity and adaption to singularities with high order of accuracy. In both cases of point-value data and of cell-average data, we are able to construct a subdivision-based algorithm producing approximations with high precision and limit functions with high piecewise regularity and without diffusion nor oscillations in the presence of discontinuities.

Key Words. Non-smooth approximation, subdivision schemes, regularity, Gibbs phenomenon, diffusion.

²This work was funded by project 20928/PI/18 (Proyecto financiado por la Comunidad Autónoma de la Región de Murcia a través de la convocatoria de Ayudas a proyectos para el desarrollo de investigación científica y técnica por grupos competitivos, incluida en el Programa Regional de Fomento de la Investigación Científica y Técnica (Plan de Actuación 2018) de la Fundación Séneca-Agencia de Ciencia y Tecnología de la Región de Murcia) and by the Spanish national research project PID2019-108336GB-I00.

^{*}Departamento de Matemática Aplicada y Estadística. Universidad Politécnica de Cartagena (Spain). e-mail: sergio.amat@upct.es

[†]School of Mathematical Sciences. Tel-Aviv University, Tel-Aviv (Israel). e-mail: levindd@gmail.com

[‡]Departamento de Matemática Aplicada y Estadística. Universidad Politécnica de Cartagena (Spain). e-mail: juan.ruiz@upct.es

1 Introduction

Subdivision schemes are very well known mathematical tools for the generation of curves and surfaces. In the past years many articles have been published about linear subdivision schemes. An incomplete list of references is, for example, [12, 16, 19, 20, 21, 24, 32, 33, 34, 35]. Non linear subdivision schemes have also attracted much attention. See for example, [5, 7, 8, 13, 27, 28, 29, 30] and the references therein for an incomplete list of publications about the subject.

Several properties of subdivision schemes are desirable for practical applications: convergence, regularity of the limit function, stability, order of approximation and adaptation to singularities. The last property usually requires the implementation of nonlinear strategies, resulting in the so called nonlinear subdivision schemes. These schemes present a regularity of the limit functions that is smaller than the one obtained by linear schemes. In practice it is usually desired that the schemes have at least C^2 regularity, as this kind of schemes are associated to improved results in the aerodynamics or hydrodynamics of the generated surface. When the data is computed with high accuracy, interpolatory subdivision schemes are preferred over approximating schemes, since using the former, the original data is preserved. These schemes are usually based on Lagrange interpolation using a centered stencil.

The ENO (Essential Non-Oscillatory) reconstruction is an approximation based on a nonlinear operator with the same order of accuracy as the linear scheme, but capable of reducing the effect of isolated singularities. It uses a selection of the stencil that aims to avoid zones affected by singularities. Thus, the precision is only reduced at the intervals which contain a singularity. The aim of the ENO subcell resolution (ENO-SR) technique is to improve the approximation properties of the reconstruction even at intervals that contain a singularity. Therefore, ENO-SR reconstruction has an improved order of accuracy over the linear reconstruction for piecewise smooth functions. In [9], the authors proposed a rigorous analysis of the ENO-SR procedure (both for the point-value and the cell-average sampling). In this article we give the details that are necessary to describe the strategy introduced in [9]. In [9], for a piecewise C^2 function f with a jump $[f']$ of the first derivative at x^* , the authors proved that the singularity is always detected for a grid-spacing discretization h smaller than the critical scale h_c being,

$$h_c := \frac{|[f']|}{4 \sup_{t \in \mathbb{R} \setminus \{x^*\}} |f''(t)|}. \quad (1)$$

This critical scale represents the minimal level of resolution needed to distinguish between the singularity and a smooth region.

The detection algorithm for the point-values sampling case in [9] can detect corner and jump discontinuities. Although, only corner singularities can be located using this discretization, as the location of jumps in the function is lost during the discretization process. Jumps in the function can be located if we use other kinds of discretization that accumulate information over the whole interval of discretization instead of sampling information at isolate locations. One example is the cell-average discretization, that we introduce later on in Section 2. In [9], the authors also perform an analysis for jump discontinuities and data discretized by cell-averages, obtaining the critical scale,

$$h_c := \frac{|[f]|}{4 \sup_{t \in \mathbb{R} \setminus \{x^*\}} |f'(t)|}, \quad (2)$$

where $[f]$ is the jump in the function f .

The algorithm for the point-values sampling is based on the comparison of second order differences for the detection of intervals that are potential candidates of containing a singularity:

$$\Delta^2 f_j = f(x_{j+1}) - 2f(x_j) + f(x_{j-1}). \quad (3)$$

Then, in [9], the intervals are labeled as B if they are suspicious of containing a singularity or G if they are not. The rules used for this process are:

1. If

$$|\Delta_h^2 f(x_{j-1})| > |\Delta_h^2 f(x_{j-1} \pm nh)|, \quad n = 1, \dots, m,$$

the intervals $I_{j-1} = [x_{j-2}, x_{j-1}]$ and $I_j = [x_{j-1}, x_j]$ are labeled as B . In this case we do not know which of the two intervals contain the singularity, so both are labeled as B .

2. If

$$|\Delta_h^2 f(x_j)| > |\Delta_h^2 f(x_j + nh)|, \quad n = 1, \dots, m-1,$$

and

$$|\Delta_h^2 f(x_{j-1})| > |\Delta_h^2 f(x_{j-1} - nh)|, \quad n = 1, \dots, m-1,$$

then the interval I_j is labeled as B . In this case, the two largest divided differences contain the interval I_j , so it is a candidate of containing the singularity.

It is assumed that the rest of the intervals do not contain a singularity. In [9] it is also proved that under the critical scale h_c presented in (1) for the point-values sampling and (2) for the cell-averages sampling, any interval that contains a singularity is labeled as B and all the intervals labeled as G are at smooth zones of the function. Even though, the algorithm can produce bad detections, i.e. intervals labeled as B at smooth regions of the function. Following [9], we can assume that given a continuous piecewise functions there exists a critical scale h_c depending only on derivatives of f at smooth regions such that all the intervals with a singularity are labeled as B or BB .

Once all the intervals have been labeled as G or B , in order to locate the position of corner singularities, we build cubic polynomials to the left and to the right of the suspicious interval, labeled as B or BB . Then, we define a function H as the difference between the two polynomials, and we suppose that there is a unique root of this function inside the suspicious interval. Note that for a sufficiently small grid-spacing, only one root of H can fall inside the considered interval. In Lemma 3, statement 2 of [9] the authors prove this fact. Thus, a good approximation for the position of the discontinuity can be easily obtained finding the roots of H . The interested reader can refer to [10] for a nice discussion about the process. The accuracy of the results depends on the order of the polynomials, as the authors prove in Lemma 3, statement 3 of [9]. In the cell-average setting, jumps in the function transform into corner singularities in the primitive and their position can be easily obtained following the process described above.

In this paper we include one step more for the location algorithm when a BB cell is detected. In this case, once we have located the discontinuity using the process described, we know which of the two contiguous B cells contains the discontinuity. Then we treat this cell as B cell and repeat the process of location in order to assure the best possible accuracy in the location of the singularity.

In [11], a specific prediction operator in the interpolatory framework was proposed and analyzed. It is oriented towards the representation of piecewise smooth continuous functions. Given a family of singularity points, a position-dependent prediction operator is defined. Its convergence was established using the matrix formalism. The algorithm lead to the successful control of the classical Gibbs phenomenon associated to the approximation of locally discontinuous functions. This position-dependent algorithm is equivalent to the ENO-SR subdivision scheme assuming the previous knowledge of the singularity positions, in particular improving the accuracy of the linear

approach.

Despite their good accuracy properties, the theoretical regularities of ENO and ENO-SR schemes are C^{1-} in the point-values, that is smaller than the regularity of the 4-point linear subdivision scheme, that is C^{2-} , as we can see in [13]. Other adaptive interpolation schemes like the PPH algorithm [2] manage to eliminate the Gibbs phenomenon close to the discontinuities, but introducing diffusion and, thus, reducing the order of accuracy but also the regularity (that is C^{1-} numerically) close to the discontinuities.

The goal of this paper is to develop a corrected implementation of the linear subdivision scheme that combines adaption to singularities and, at the same time, high order of regularity avoiding diffusion and Gibbs phenomenon. Indeed, we present a procedure to develop corrected subdivision approximations for functions with discontinuities which have the five important properties:

1. Interpolation.
2. High precision.
3. High piecewise regularity.
4. No diffusion.
5. No oscillations

As far as we know, this is the first time that subdivision schemes that own all these properties at the same time appear in the literature. We present the particular case of the 4-point Dubuc-Deslauriers interpolatory subdivision scheme [15] through which we obtain a C^{2-} piecewise regular limit function and that is capable of reproducing piecewise cubic polynomials. Indeed, it is straightforward to obtain higher regularity and reproduction of piecewise polynomials of higher degree, just using the same technique with larger stencils. It is also possible and straightforward to extend the correction construction presented in this article to other subdivisions schemes aimed to deal with data that contain singularities.

The paper is organized as follows: in Section 2 we introduce the discretizations that is being used in the paper, Section 3 is dedicated to introduce our corrected approximation approach, and the analysis of the approximation order of the resulting approximants. Section 4 is dedicated to check that the numerical regularity of the limit function in the point-values and the cell-average discretization corresponds to the one found theoretically. In Section 5 we present some experiments for univariate and bivariate functions discretized by point-values' sampling, in Section 6 we show some experiments for univariate and bivariate functions discretized by cell-averages' sampling and, finally, in Section 7 we expose the conclusions.

2 The discretizations: point-values and cell averages

In the case of a point-values discretization we can just consider that we are given a vector of values on a grid. This means that our data is interpreted as the sampling of a function at grid-points $\{x_j = jh\}$. In this case, as it has been mentioned above, the position of the discontinuities in the function is lost during the discretization process and there is no hope to recover their exact position. Other kind of singularities, such as discontinuities in the first derivative, can be located using the point-values discretization. Another option is to consider the original data as averages of a certain piecewise continuous function over the intervals of a grid. This is the cell-average setting, which also allows to locate jump discontinuities in the function. In both cases we consider the grid points in $[0, 1]$:

$$X = \{x_j\}_{j=0}^N, \quad x_j = jh, \quad h = \frac{1}{N}.$$

For the point-values case we use the discretization $\{f_j = f(x_j)\}_{j=0}^N$ at the data points $\{x_j = jh\}_{j=0}^N$.

On the other hand, for the cell-averages sampling we are given the local averages values,

$$\bar{f}_j = \frac{1}{h} \int_{x_{j-1}}^{x_j} f(x) dx, \quad j = 1, \dots, N. \quad (4)$$

Also in this case we aim at approximating the underlying function f .

Let us define the sequence $\{F_j\}$ as,

$$F_j = h \sum_{i=1}^j \bar{f}_i = \int_0^{x_j} f(y) dy, \quad j = 1, \dots, N, \quad (5)$$

taking $F_0 = 0$. Denoting by F the primitive function of f , i.e. $F(x) = \int_0^x f(y) dy$, the values $\{F_j\}$ are the point-values discretization of F . Now we are back in the case of point-value data, for F , and after finding an approximation $G(x)$ to $F(x)$, $g(x) = G'(x)$ would be the approximation to $f(x) = F'(x)$, such that,

$$\bar{g}_j = \frac{F_j - F_{j-1}}{h}. \quad (6)$$

In the following sections we suggest the framework of a corrected subdivision algorithm that is adapted to the discontinuities, that avoids the Gibbs phenomenon, that attains the same regularity at smooth zones as the equivalent linear algorithm, without diffusion and that reproduces polynomials of the degree associated to the linear scheme used.

3 A corrected implementation of linear subdivision schemes

We present our approach for the approximation of a function with one singular point. Later on we explain how to use it for the case of several singular points.

Let f be a piecewise C^4 -smooth function on $[0, 1]$, with a singular point at x^* , and assume we are given the vector of values $\{f(x_i)\}_{i=0}^N$ at the data points $\{x_i = ih\}_{i=0}^N$, $N = 1 + 1/h$. We denote by $f^-(x)$ and $f^+(x)$ the functions to the left and to the right of the discontinuity respectively.

In our framework we are going to use the 4-point Dubuc-Deslauriers subdivision scheme:

$$\begin{cases} (Sf^k)_{2j} = f_j^k, \\ (Sf^k)_{2j+1} = -\frac{1}{16}f_{j-1}^k + \frac{9}{16}f_j^k + \frac{9}{16}f_{j+1}^k - \frac{1}{16}f_{j+2}^k. \end{cases} \quad (7)$$

This scheme has fourth order of accuracy for C^4 functions, and it has a C^{2-} regularity [15], [17]. We aim at retrieving these properties for functions with jump singularities in the function and the first derivative for data discretized by point-values or by cell-averages.

3.1 The corrected approximation algorithm for point-values data

In this subsection we introduce the corrected approximation algorithm. Let $T_3^-(x)$ and $T_3^+(x)$ be the third order Taylor approximations of f^- and of f^+ at x^* respectively. Consider the one sided cubic polynomial

$$\begin{cases} T_+(x) = 0, & x < x^*, \\ T_+(x) = T_3^+(x) - T_3^-(x), & x \geq x^*. \end{cases} \quad (8)$$

For $x \geq x^*$

$$T_+(x) = [f] + [f'](x - x^*) + \frac{1}{2}[f''](x - x^*)^2 + \frac{1}{6}[f'''](x - x^*)^3, \quad (9)$$

where $[f]$, $[f']$, $[f'']$, $[f''']$ denote the jumps in the derivatives of f at x^* : $[f] = f^+(x^*) - f^-(x^*)$, $[f'] = (f^+)'(x^*) - (f^-)'(x^*)$, $[f''] = (f^+)''(x^*) - (f^-)''(x^*)$ and $[f'''] = (f^+)'''(x^*) - (f^-)'''(x^*)$.

It follows that

$$g \equiv f - T_+ \in C^3[0, 1],$$

and this observation is the basis for our proposed algorithm. Since we do not know the exact left and right derivatives of f at x^* , we will use instead a fourth order approximation of $T_+(x)$: For $x \geq x^*$,

$$\tilde{T}_+(x) = \widetilde{[f]} + \widetilde{[f']}(x - x^*) + \frac{1}{2}\widetilde{[f'']}(x - x^*)^2 + \frac{1}{6}\widetilde{[f''']}(x - x^*)^3, \quad (10)$$

where

$$\begin{pmatrix} \widetilde{[f]} \\ \widetilde{[f']} \\ \widetilde{[f'']} \\ \widetilde{[f''']} \end{pmatrix} = \begin{pmatrix} [f] \\ [f'] \\ [f''] \\ [f'''] \end{pmatrix} + \begin{pmatrix} O(h^4) \\ O(h^3) \\ O(h^2) \\ O(h) \end{pmatrix}. \quad (11)$$

Note that near $x = x^*$, i.e., if $|x - x^*| = O(h)$,

$$|T_+(x) - \tilde{T}_+(x)| = O(h^4), \quad \text{as } h \rightarrow 0. \quad (12)$$

Our algorithm has three steps:

- **Step 1:** Smoothing the data.

We compute the new data using $\tilde{T}_+(x)$ in (10),

$$\tilde{g}(x_i) = f(x_i) - \tilde{T}_+(x_i), \quad i = 0, \dots, N. \quad (13)$$

It is clear that $g(x)$ does not present singularities up to the third derivative. As we show below, using a fourth order approximation \tilde{g} to g , implies a truncation error that is $O(h^4)$.

- **Step 2:** Subdivision.

We apply the 4-point interpolatory subdivision scheme to the data $\tilde{g}(x_j)$ and we denote the limit function by \tilde{g}^∞ .

- **Step 3:** Correcting the approximation.

$$\tilde{f}^\infty(x) = \tilde{g}^\infty(x) + \tilde{T}_+(x) \quad (14)$$

In Figure 1 we present an example with one of the functions that we use in the numerical experiments (more specifically, the one in (25)). The circles represent a function discretized by point-values with a discontinuity in the first derivative. The dots represent the smoothed data in (13), and

we can see that it owns better regularity properties than the original data. Using the strategy presented in this section, we apply a subdivision scheme to the corrected data and then we compute the corrected approximation in (14).

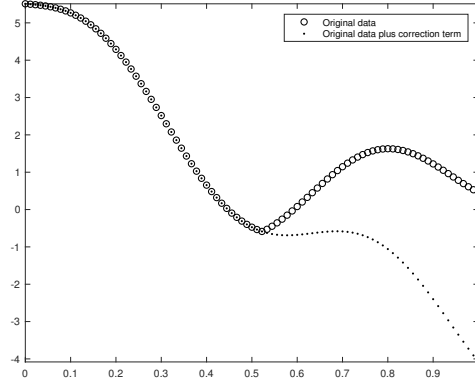


Figure 1: The circles in this graphs correspond to the original data obtained from the discretization of the function in (25). The dots correspond to the corrected data in (13).

Remark 1. *It is important to note here that the algorithm can be applied to functions with $m > 1$ discontinuities. In this case the correction can be applied iteratively from left to right as the discontinuities are found. The total correction term would be,*

$$\tilde{T}_+^{total}(x) = \sum_{n=1}^m \tilde{T}_+^n(x),$$

being

$$\tilde{T}_+^n(x) = \widetilde{[f]}_n + \widetilde{[f']}_n(x - x_n^*) + \frac{1}{2}\widetilde{[f'']}_n(x - x_n^*)^2 + \frac{1}{6}\widetilde{[f''']}_n(x - x_n^*)^3, \quad (15)$$

the correction term (10) at each of the m discontinuities placed at $x_n^*, n = 1, \dots, m$, found in the data. In this case, $\tilde{T}_+^{total}(x)$ should be used instead on $\tilde{T}_+(x)$ in steps 1 and 3 of the algorithm.

3.2 The approximation algorithm for cell-averages data

In order to work with data discretized by cell-averages, $\{\bar{f}_j\}$, we firstly obtain the point-values $\{F_j\}$ of the primitive function F (5). Then we apply

our strategy for the point-values discretization described above to obtain an approximation $G \sim F$ and then approximate f by G' . The main difference from the case of point-values data is that the function F is a continuous function, with a jump in its first derivative. Thus, an additional step in the algorithm for cell-averages data is to define x^* as the intersection point of the two local polynomials derived from the data $\{F_j\}$. In Figure 2 we represent this process.

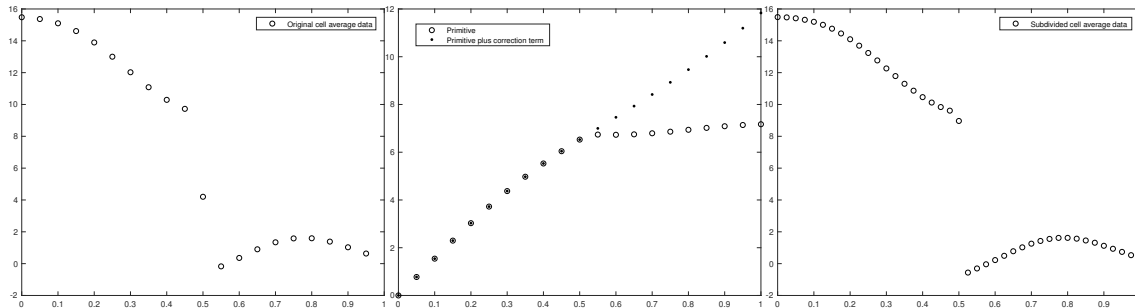


Figure 2: Left, primitive of the function presented in (30). Center, primitive of the data in the plot to the left, and the corrected primitive. Right, result of the subdivision of the function discretized by cell-averages.

In the next section we present the construction of a fourth order accurate approximation of the jumps in the function and its derivatives for data discretized by point-values.

3.3 Accurate approximation of the jumps in the function and its derivatives

The approximation of the jumps with the desired accuracy can be obtained using the strategy derived by us in [1]. In order to obtain the approximate jumps in the derivatives of f we need to know the position of the discontinuity x^* up to certain accuracy. In the introduction we mentioned how to obtain an approximation of the position of the discontinuity x^* with the desired accuracy following [9]. If we work with stencils of four points, we need $O(h^4)$ accuracy in the detection. Let's suppose that we know that the discontinuity is placed at a distance α from x_j in the interval $\{x_j, x_{j+1}\}$. If we want $O(h^4)$ accuracy for the approximation of the jump relations, we need to use four points to each side of the discontinuity. Let's suppose that we use the stencil $\{f_{j-3}^+, f_{j-2}^+, f_{j-1}^+, f_j^+, f_{j+1}^-, f_{j+2}^-, f_{j+3}^-, f_{j+4}^-\}$ placed at the

positions $\{x_{j-3}, x_{j-2}, x_{j-1}, x_j, x_{j+1}, x_{j+2}, x_{j+3}, x_{j+4}\}$. Then, we can approximate the values of the derivatives of f from both sides of the discontinuity just using third order Taylor expansion around x^* and setting the following system of equations for the $-$ side,

$$\begin{aligned} f_j^- &= f^-(x^*) - f_x^-(x^*)\alpha + \frac{1}{2}f_{xx}^-(x^*)\alpha^2 - \frac{1}{3!}f_{xxx}^-(x^*)\alpha^3, \\ f_{j-1}^- &= f^-(x^*) - f_x^-(x^*)(h+\alpha) + \frac{1}{2}f_{xx}^-(x^*)(h+\alpha)^2 - \frac{1}{3!}f_{xxx}^-(x^*)(h+\alpha)^3, \\ f_{j-2}^- &= f^-(x^*) - f_x^-(x^*)(2h+\alpha) + \frac{1}{2}f_{xx}^-(x^*)(2h+\alpha)^2 - \frac{1}{3!}f_{xxx}^-(x^*)(2h+\alpha)^3, \\ f_{j-3}^- &= f^-(x^*) - f_x^-(x^*)(3h+\alpha) + \frac{1}{2}f_{xx}^-(x^*)(3h+\alpha)^2 - \frac{1}{3!}f_{xxx}^-(x^*)(3h+\alpha)^3, \end{aligned} \quad (16)$$

and for the $+$ side,

$$\begin{aligned} f_{j+1}^+ &= f^+(x^*) + f_x^+(x^*)(h-\alpha) + \frac{1}{2}f_{xx}^+(x^*)(h-\alpha)^2 + \frac{1}{3!}f_{xxx}^+(x^*)(h-\alpha)^3, \\ f_{j+2}^+ &= f^+(x^*) + f_x^+(x^*)(2h-\alpha) + \frac{1}{2}f_{xx}^+(x^*)(2h-\alpha)^2 + \frac{1}{3!}f_{xxx}^+(x^*)(2h-\alpha)^3, \\ f_{j+3}^+ &= f^+(x^*) + f_x^+(x^*)(3h-\alpha) + \frac{1}{2}f_{xx}^+(x^*)(3h-\alpha)^2 + \frac{1}{3!}f_{xxx}^+(x^*)(3h-\alpha)^3, \\ f_{j+4}^+ &= f^+(x^*) + f_x^+(x^*)(4h-\alpha) + \frac{1}{2}f_{xx}^+(x^*)(4h-\alpha)^2 + \frac{1}{3!}f_{xxx}^+(x^*)(4h-\alpha)^3, \end{aligned} \quad (17)$$

being $\alpha = x^* - x_j$. It is clear that the previous systems can be written in matrix form where the system matrix is a Vandermonde matrix, that is always invertible.

Solving the two systems (16) and (17), where $f^-(x^*)$, $f_x^-(x^*)$, $f_{xx}^-(x^*)$, $f_{xxx}^-(x^*)$ and $f^+(x^*)$, $f_x^+(x^*)$, $f_{xx}^+(x^*)$, $f_{xxx}^+(x^*)$ are the unknowns, we can obtain approximations for the jumps in the derivatives of f .

It is easy to prove [1] that

$$\begin{pmatrix} \widetilde{[f]} \\ \widetilde{[f']} \\ \widetilde{[f'']} \\ \widetilde{[f''']} \end{pmatrix} = \begin{pmatrix} f^+(x^*) - f^-(x^*) \\ f_x^+(x^*) - f_x^-(x^*) \\ f_{xx}^+(x^*) - f_{xx}^-(x^*) \\ f_{xxx}^+(x^*) - f_{xxx}^-(x^*) \end{pmatrix} + \begin{pmatrix} O(h^4) \\ O(h^3) \\ O(h^2) \\ O(h) \end{pmatrix}. \quad (18)$$

3.4 The approximation properties

Let us analyze the approximation properties of the corrected scheme for the case of point-values data and for cell-averages data.

It is important to note that the technique described in this and previous sections can also be applied to treat the approximation near the boundary points 0 and 1. Outside the boundary we use a zero padding strategy, and we treat each boundary as a discontinuity which position is known. Thus, treating the boundaries is just considering more than one discontinuity in the data, as explained in Remark 1. Using this strategy enables us to extend the approximation results discussed below to the entire interval $[0, 1]$. In the following we implicitly assume that the boundaries are treated as above.

For the point-values' case we consider that a discontinuity is placed in the interval (x_j, x_{j+1}) . For the point-values discretization, we will consider two cases: when we find jumps in the function or in the first derivative. Let's start by the former.

We are working with jump discontinuities in the point-values so, strictly, we can not know the exact location of the discontinuity. Thus, we can only hope to obtain a limit function that contains a jump discontinuity in the same interval as the original function. As the exact location of the discontinuity is an information that can not be obtained by any means from the data, we can just assume that the approximated location of the discontinuity corresponds with the exact location of the discontinuity.

Theorem 3.1. - The point-values' case: jump discontinuities. *Let f be a piecewise C^4 -smooth function on $[0, 1]$, with a jump discontinuity, and assume we are given the vector of values $\{f_j\}_{j=0}^N$ at the data points $\{x_j = jh\}_{j=0}^N$, $N = 1 + 1/h$. Let's choose the singular point to be at $x^* \in (x_j, x_{j+1})$. Then the corrected approximation obtained by the corrected algorithm interpolates the data points, it is $C^{2-}([0, x^*) \cup (x^*, 1])$, and $\|f - \tilde{f}^\infty\|_{\infty, [0, 1] \setminus \{x^*\}} = O(h^4)$ as $h \rightarrow 0$, for any piecewise C^4 -smooth f that has a singular point at x^* and that has as point-values $\{f(x_j)\}_{j=0}^N = \{f_j\}_{j=0}^N$.*

Proof. The 4-point subdivision scheme is an interpolatory scheme and the limit function it defines is C^{2-} [15]. Hence,

$$\tilde{g}^\infty(x_j) = f(x_j) - \tilde{T}_+(x_j),$$

and $\tilde{g}^\infty \in C^{2-}[0, 1]$. Adding the correction term in (14) yields the interpolation to f and the smoothness property.

To prove the approximation order, we use the fact that the subdivision scheme is a local procedure and that it reproduces cubic polynomials. Furthermore, by [15], [17], for $f \in C^4(\mathbb{R})$ the 4-point subdivision scheme gives $O(h^4)$ approximation order to f . Therefore, away from the singularity, for $x < x_{j-2}$ and for $x > x_{j+3}$,

$$|\tilde{g}^\infty - (f - \tilde{T}_+)| = O(h^4),$$

as $h \rightarrow 0$. Correcting the approximation by \tilde{T}_+ yields the approximation result away from x^* .

To show the approximation order near x^* , we rewrite the data for the subdivision process, $\tilde{g}(x_j) = f(x_j) - \tilde{T}_+(x_j)$, as

$$\tilde{g}(x_j) = f(x_j) - T_+(x_j) - T_3^-(x_j) + (T_+(x_j) - \tilde{T}_+(x_j)) + T_3^-(x_j).$$

Denoting $q = f - T_+ - T_3^-$, we observe that $q = f - T_3^-$ for $x < x^*$ and $q = f - T_3^+$ for $x > x^*$. In both cases $q(x) = O(h^4)$ near x^* . Next we note that by (11)

$$(T_+(x_i) - \tilde{T}_+(x_i)) = O(h^4),$$

for $i - 4 \leq j \leq i + 5$. Using the above, plus the locality of the subdivision scheme and the reproduction of cubic polynomials, it follows that

$$\tilde{g}^\infty(x) = T_3^-(x) + O(h^4), \quad x_{j-2} \leq x \leq x_{j+3}.$$

Finally, in view of (8) and (12) we obtain

$$\tilde{f}^\infty(x) = \tilde{g}^\infty(x) + \tilde{T}_+(x) = \begin{cases} T_3^-(x) + O(h^4), & x_{j-2} \leq x \leq x^*, \\ T_3^+(x) + O(h^4), & x^* \leq x \leq x_{j+3}, \end{cases} \quad (19)$$

implying that

$$\tilde{f}^\infty(x) = f(x) + O(h^4), \quad x_{j-2} \leq x \leq x_{j+3}, \quad x \neq x^*,$$

which completes the proof. \square

Remark 2. *In order to include the point x^* in Theorem 3.1, we need to suppose that the initial data comes from a function that is continuous from the left or from the right of x^* , as this information, as well as the exact position of the discontinuity is lost in the discretization process.*

Now we can continue with the case when we find corner singularities, i.e. discontinuities in the first derivative.

Theorem 3.2. - The point-values' case: discontinuities in the first derivative. *Let f be a piecewise C^4 -smooth function on $[0, 1]$, with a jump discontinuity in the first derivative, and assume we are given the vector of values $\{f_j\}_{j=0}^N$ at the data points $\{x_j = jh\}_{j=0}^N$, $N = 1 + 1/h$. Let's suppose that the singular point is placed at $s^* \in (x_j, x_{j+1})$ and that we have located the singularity at the approximated location $x^* \in (x_j, x_{j+1})$. Then, the corrected approximation obtained by the corrected algorithm interpolates the data points, it is C^{2-} on $[0, x^*) \cup (x^*, 1]$, and $\|f - \tilde{f}^\infty\|_\infty = O(h^4)$ as $h \rightarrow 0$.*

Proof. Outside the interval (x^*, s^*) (if the approximated location x^* is to the right of s^* , the analysis is equivalent), the proof is similar to the one followed in Theorem 3.1.

Let's now analyze the case when we subdivide in the interval (x^*, s^*) . We can just follow the proof of Theorem 1 in [9]. We suppose that the discontinuity is placed in the interval $[x_j, x_{j+1}]$, being $h = x_{j+1} - x_j$ a uniform grid-spacing. A graph of this case is plotted in Figure, 3. As we are using cubic polynomials for the location of the discontinuity, it is clear that the distance between x^* and s^* must be $O(h^4)$, as proved in statement 3 of Lemma 3 of [9]. Let us analyze the accuracy attained by the subdivision scheme in the point-values discretization in the interval (x^*, s^*) . The left side of the discontinuity placed at s^* is labeled as the $-$ side and the right side of s^* as the $+$ side. The approximated location of the discontinuity is labeled as x^* . Following the process described in Section 3.3 we obtain the jumps in the function and its derivatives at x^* . It is clear that if the piecewise function is not composed of polynomials of degree smaller or equal than 3, the location of the discontinuity will be approximated. In this case, obtaining the jump in the function and its derivatives at x^* is just as extending f^+ from s^* up to x^* , as shown in Figure 3. Let's write the limit function obtained by the corrected algorithm as,

$$\tilde{f}^\infty(x) = \begin{cases} (\tilde{f}^\infty)^-(x) & x < x^*, \\ (\tilde{f}^\infty)^+(x) & x > x^*. \end{cases} \quad (20)$$

The error obtained at any point $x \in (x^*, s^*)$ will be,

$$|f(x) - \tilde{f}^\infty(x)| = |f^-(x) - (\tilde{f}^\infty)^+(x)| \leq |f^-(x) - f^+(x)| + |f^+(x) - (\tilde{f}^\infty)^+(x)|. \quad (21)$$

Following similar arguments to the ones used in the first part of the proof, the second term is bounded and is $O(h^4)$. For the first term, we can use second order Taylor expansion around s^* to write,

$$|f^-(x) - f^+(x)| \leq |[f']|(s^* - x) + \sup_{\mathbb{R} \setminus s^*} |f''|(s^* - x)^2 \leq (s^* - x^*) \left(|[f']| + \sup_{\mathbb{R} \setminus s^*} |f''| h \right). \quad (22)$$

As $h < h_c$ (see (1)), then

$$|f^-(x) - f^+(x)| \leq \frac{5}{4} |[f']|(s^* - x^*). \quad (23)$$

Now, we can use point 3 of Lemma 2 of [9], that establishes that $(s^* - x^*) \leq C \frac{h^m \sup_{x \in \mathbb{R} \setminus \{s^*\}} |f^{(m)}(x)|}{|[f']|}$ (with $m = 4$ in our case), to obtain that the first term

of the right hand side of (21) is also bounded and is $O(h^4)$. This concludes the proof. \square

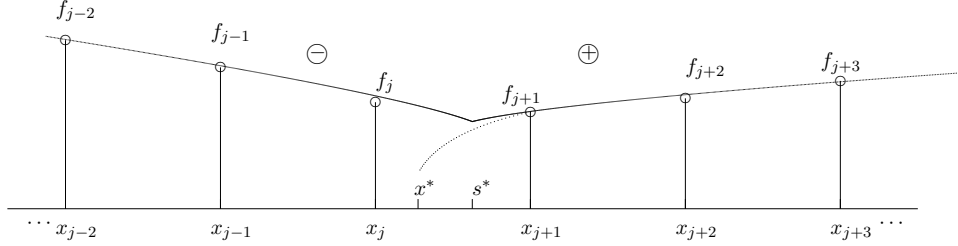


Figure 3: In this figure we can see an example of a corner singularity placed in the interval (x_j, x_{j+1}) , being $h = x_{j+1} - x_j$ a uniform grid-spacing. The left side of the discontinuity placed at s^* is labeled as the $-$ side and the right side of s^* as the $+$ side. The approximated location of the discontinuity is labeled as x^* .

Due to the order of accuracy attained by the corrected algorithm close to the discontinuity and to the regularity and convergence of the linear scheme we can state the following corollary:

Corollary 3.3. *The corrected subdivision scheme does not introduce Gibbs phenomenon nor diffusion close to the discontinuities.*

Proof. Given the fact that the correction introduced in step 1 of the algorithm eliminates the presence of the discontinuity up to the order of accuracy of the linear scheme, we can consider that the linear scheme in step 2 is applied to smooth data after the correction, so no Gibbs effect can appear. Step 3 consists in correcting back the subdivided data, so no diffusion can appear. \square

Corollary 3.4. *The corrected subdivision scheme reproduces piecewise cubic polynomials.*

Proof. For piecewise cubic polynomials, the location of the discontinuity is exact. Remind that we are using cubic interpolating polynomials for the location algorithm. Following Theorem 3.1 we get the proof. Mind that if the singularity is in the first derivative, the proof given for Theorem 3.1 would be equivalent for this case, as now we know that the exact position of the singularity is x^* . \square

In what follows, we enumerate the main properties of the corrected algorithm:

- The corrected subdivision scheme has the same (piecewise) regularity as the linear subdivision used.
- The corrected subdivision scheme does not produce any oscillations in the presence of singularities.
- The algorithm has high accuracy without diffusion.
- The algorithm is interpolatory.
- The corrected subdivision scheme is exact for piecewise polynomial functions of the same degree as the one used in the construction of the scheme.
- The corrected subdivision scheme is stable due to the stability of the linear scheme used.

Let's consider now the cell-averages discretization. In this case, we will only analyze the detection of jumps in the function.

Theorem 3.5. - The cell-averages' case. *Let f be a piecewise C^3 -smooth function on $[0, 1]$, with a jump discontinuity at s^* , and assume we are given the cell-averages*

$$\bar{f}_j = \frac{1}{h} \int_{x_{j-1}}^{x_j} f(x) dx, \quad j = 1, \dots, N.$$

Using the algorithm in Section 3.2, the following results hold:

1. *The approximate singular point x^* satisfies $|s^* - x^*| \leq Ch^4$.*
2. *The approximation $G(x)$ to the primitive function $F(x)$ interpolates the data $\{F_j\}_{j=1}^N$, and $|F(x) - G(x)| \leq Ch^4$, $x \in [0, 1]$.*
3. *The approximation $g(x) = G'(x)$ to $f(x)$ satisfies $|f(x) - g(x)| = O(h^3)$ as $h \rightarrow 0$ for $x \in [0, 1]$, x not in the closed interval between s^* and x^* .*
4. *Denoting $\delta = x^* - s^*$,*

$$|f(x) - g(x + \delta)| \leq Ch^3 \quad \forall x \in [0, 1] \setminus \{s^*\}.$$

Proof. Figure 4 represents a possible scenario for this theorem. Let us prove every point of the theorem:

1. First we note that the primitive function F is piecewise C^4 . After locating the interval $[x_j, x_{j+1}]$ containing the singular point, the algorithm finds the two cubic polynomials, \tilde{T}_- and \tilde{T}_+ , respectively interpolating the data at four points to the left and to the right of the singularity interval. As we are using cubic polynomials for the location of the singularity, the intersection point x^* of the two polynomials in $[x_j, x_{j+1}]$ satisfies $|s^* - x^*| \leq Ch^4$, as proved in point 3 of Lemma 3 of [9].
2. Now we can follow the steps of Theorem 3.1 to deduce that $|F(x) - G(x)| \leq Ch^4$, $x \in [0, 1]$.
3. We also use here the result in [31] that for $F \in C^4(\mathbb{R})$ the 4-point subdivision scheme gives $O(h^3)$ approximation order to the derivative of F . This, together with the observation that both F and G are differentiable outside the interval between s^* and x^* , yield the result in item 3.
4. To prove item 4 let us assume, w.l.o.g., that $x^* > s^*$. Both f and $g(\cdot + \delta)$ have their jump discontinuity at s^* . For $x < s^*$ we have $x + \delta < x^*$. Since $|\delta| = O(h^4)$, and g is continuous for $x < x^*$, it follows that

$$g(x + \delta) = g(x) + O(h^4).$$

Hence,

$$|f(x) - g(x + \delta)| = |f(x) - g(x)| + O(h^4),$$

and by item 3, $|f(x) - g(x)| = O(h^3)$. Similarly, for $x > s^*$, $x + \delta > x^*$ and $|f(x + \delta) - f(x)| = O(h^4)$. Hence,

$$|f(x) - g(x + \delta)| = |f(x + \delta) - g(x + \delta)| + O(h^4) = O(h^3).$$

□

Remark 3. Inside the interval between s^* and x^* , as mentioned in Section 7 of [9], we can not hope to obtain a better accuracy than $O(1)$ in the infinity norm. Even though, we can provide a result in the L^1 norm (in fact, this result is provided for the L^p norm in Section 7 of [9]) having into account that,

$$\|f^\infty - f\|_{L^1} \leq \|f^\infty - g\|_{L^1} + \|g - f\|_{L^1},$$

where f^∞ is the limit function in the cell-averages and g is the smooth function obtained by our algorithm plus the final translation, which has the

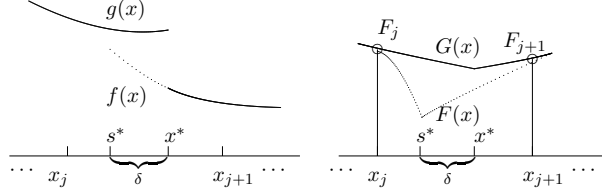


Figure 4: In this figure we represent a jump discontinuity in the interval (x_j, x_{j+1}) , that transforms into a discontinuity in the first derivative for the primitive. The approximated location of the discontinuity is labeled as x^* and the exact location is labeled as s^* . The exact function is represented by $f(x)$ and the approximation is represented by $g(x)$. The exact primitive is represented by $F(x)$ and the approximation is represented by $G(x)$.

same cell-averages as the function f and has the discontinuity at x^* . The first term of the right hand side of the inequality is controlled by the order of the linear subdivision scheme (as the correction do not perturb the order) and the second term is controlled using the results in Section 7 of [9].

4 Numerical regularity of the limit function for data discretized by point-values or by averages

We would like to check numerically the regularity of the data provided by the corrected subdivision scheme, that is inherited from the linear subdivision scheme used. We also want to compare it with the numerical regularity provided by the ENO-SR method. Thus, an appropriate estimate for the regularity of a subdivision scheme in the point-values or the cell-averages should be used. We start by providing the definition of Hölder regularity:

Definition 4.1. An l times continuously differentiable function $f : \Omega \subset \mathbb{R} \rightarrow \mathbb{R}$ is said to have Hölder regularity $R_H = l + \alpha$, if

$$\exists C < \infty \text{ such that } \left| \frac{\partial^l f(y)}{\partial x^l} - \frac{\partial^l f(z)}{\partial x^l} \right| \leq C|y - z|^\alpha, \forall y, z \in \Omega$$

Remark 4. It is clear that if we apply this definition to the primitive $F = \int_a^x f(x)dx$ of f , the value of l will be reduced by one and the regularity of f will result one order lower than the regularity of F .

In [23] it is given a definition for the regularity of a subdivision scheme in the point-value case, considering that Δx_i are divided differences and $\Delta^2 x_i$ are second divided differences:

Definition 4.2. A C^l subdivision scheme for the point-values is said to have Hölder regularity $l + \alpha_l$, if

$$\exists C < \infty \text{ such that } \lim_{l \rightarrow \infty} l! \left| \Delta^l f_{j+1}^k - \Delta^l f_j^k \right| \leq C(2^{-k}h)^{\alpha_l},$$

If $\alpha_l = 1$, this definition implies that the subdivision scheme is almost C^{l+1} . In Section 2 we explained that working with the cell-averages of a function, it is possible to obtain the exact point-values of the primitive. Then, we can just measure the regularity of the function f discretized through cell-averages using the regularity of the primitive.

Definition 4.3. The subdivision scheme in the point-values for the primitive F is said to have Hölder regularity $l + \alpha_l$ if

$$\exists C < \infty \text{ such that } \lim_{l \rightarrow \infty} l! \left| \Delta^l F_{j+1}^k - \Delta^l F_j^k \right| \leq C(2^{-k}h)^{\alpha_l},$$

and this means that the subdivision scheme for the cell-averages of f has Hölder regularity $l - 1 + \alpha_l$, as

$$\left| \Delta^l F_{j+1}^k - \Delta^l F_j^k \right| = \left| \Delta^{l-1} f_{j+1}^k - \Delta^{l-1} f_j^k \right|,$$

Then, following [23], the regularity of a limit function obtained through point-values or cell-averages can be evaluated numerically. Using S_1 and S_2 , the subdivision schemes for the (undivided) differences of order $l = 1$ and $l = 2$ associated to the subdivision scheme S , the following quantities are estimated for $l = 1, 2$ and different values of the subdivision level j :

$$\alpha_l = -\log_2 \left(2^l \frac{\|(S_l^{k+1}f)_{j+1} - (S_l^{k+1}f)_j\|_\infty}{\|(S_l^k f)_{j+1} - (S_l^k f)_j\|_\infty} \right). \quad (24)$$

This expression provides an estimate for α_1 and α_2 such that the limit functions belong to $C^{1+\beta_1-}$ and $C^{2+\beta_2-}$ if the data is discretized in the point-values. On the other hand, for the case of cell-averages data, we just have to apply the expression in (24) to the values of the primitive F . In this case, the limit function belongs to C^{β_1-} and $C^{1+\beta_2-}$. Mind that we have only deducted one from the regularity of the limit function for the primitive.

5 Numerical results for the case of point-values sampling

In the experiments presented in this section we have calculated a high accuracy approximation of the position of the discontinuity using the technique described in the introduction. We have also computed high order approximations of the jumps in the function and its derivatives using the process described in Section 3.3.

Let's start by the function,

$$f(x) = \begin{cases} a + (x - \frac{\pi}{6})(x - \frac{\pi}{6} - 10) + x^2 + \sin(10x), & \text{if } x < \frac{\pi}{6} \\ x^2 + \sin(10x), & \text{if } x \geq \frac{\pi}{6}, \end{cases} \quad (25)$$

with $a = 0$ and $x \in [0, 1]$. It is easy to check that the jump in the function at $x = \frac{\pi}{6}$ is $[f(x = \pi/6)] = 0$, the jump in the first derivative is $[f'(x = \pi/6)] = 10$ and in the second derivative is $[f''(x = \pi/6)] = -2$.

In Figure 5 we present the result obtained by the linear algorithm (left), the quasi-linear ENO-SR scheme (center) and the corrected algorithm (right). In Figure 6 we present a zoom around the singularity. In order to obtain these graphs we have started from 16 data points of the original function and we have performed 5 levels of subdivision. We represent the original function with a dotted line, the discretized data at the lower resolution (16 data points) with blank circles and the limit function with a dashed line. We can see that the results obtained by the quasi-linear algorithm and the corrected algorithm are very similar. Even though, as we will see in Subsection 5.2, the regularity of the limit function obtained by the quasi-linear algorithm is lower than the one obtained by the corrected approach.

Now we apply the algorithm to a function with more than one discontinuity. For example, the function

$$f(x) = \begin{cases} (x - \frac{\pi}{12})(x - \frac{\pi}{12} - 10) + x^2 + \sin(10x), & \text{if } x < \frac{\pi}{6} \\ x^2 + \sin(10x), & \text{if } \frac{\pi}{12} \leq x < \frac{3\pi}{12} \\ (x - \frac{3\pi}{12})(x - \frac{3\pi}{12} - 5) + x^2 + \sin(10x), & \text{if } x \geq \frac{3\pi}{12}, \end{cases} \quad (26)$$

that presents two discontinuities. In Figure 7 we present the result obtained when applying the corrected algorithm to the function in (26). We can see that the algorithm can deal with more than one discontinuity with no problem, just applying steps 1 and 3 of Section 3 as many times as discontinuities are detected.

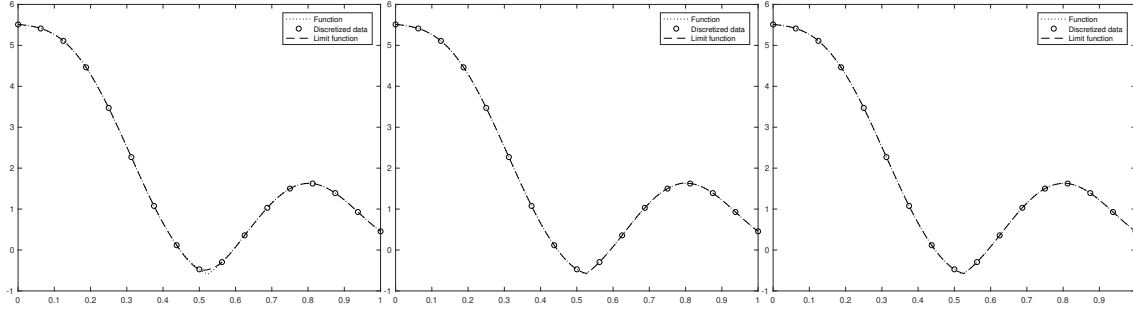


Figure 5: Limit function obtained by the linear algorithm (left), the quasi-linear algorithm (center) and the corrected algorithm (right). In order to obtain these graphs we have started from 16 initial data points of the function in (25).

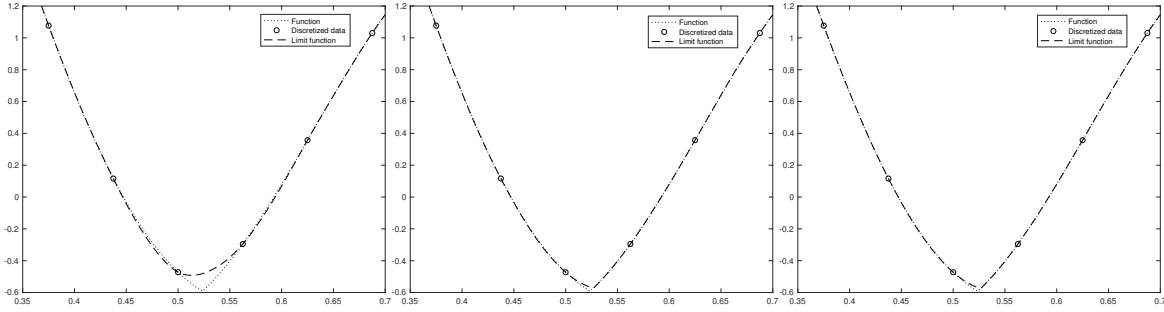


Figure 6: Zoom of the limit functions shown in Figure 5 obtained by the linear algorithm (left), the quasi-linear algorithm (center) and the corrected algorithm (right).

5.1 Jump discontinuities in the point-values sampling case

We have previously mentioned that it is not possible to locate the position of a discontinuity in the function using a discretization by point-values. Although this is true, it is indeed possible to locate the interval of length h that contains the discontinuity. Our objective is to obtain subdivided data that keeps the regularity of the linear subdivision scheme applied, that does not present diffusion nor Gibbs phenomenon and that have optimal accuracy close to the discontinuities. Then, as argued in Theorem 3.1, we just assume that the discontinuity is placed at the middle of the interval. Let's apply the corrected subdivision algorithm to data obtained from the sampling of

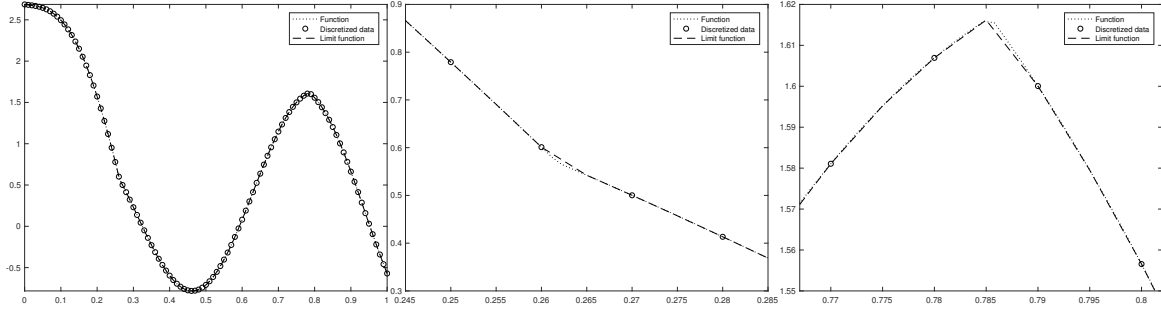


Figure 7: Limit function obtained by the corrected algorithm after five levels of subdivision using as initial data the piecewise smooth function in (26) that presents two singularities.

the function,

$$f(x) = \begin{cases} \left(x - \frac{\pi}{12}\right) \left(x - \frac{\pi}{12} - 10\right) + x^2 + \sin(10x) + 1, & \text{if } x < \frac{\pi}{6}, \\ x^2 + \sin(10x), & \text{if } \frac{\pi}{12} \leq x < \frac{3\pi}{12}, \\ \left(x - \frac{3\pi}{12}\right) \left(x - \frac{3\pi}{12} - 5\right) + x^2 + \sin(10x) + 2, & \text{if } x \geq \frac{3\pi}{12}. \end{cases} \quad (27)$$

Figure 8 presents the result obtained after five levels of subdivision using 100 initial points. As expected, we do not obtain Gibbs phenomenon nor diffusion. It is important to mention that in Figure 8 we have plotted the limit function and the original data with continuous lines to point out the position of the jump in the function, but no data or subdivided data is placed in the middle of the jump.

In the following subsections we will check the regularity and the accuracy obtained using the corrected algorithm.

5.2 Numerical Regularity

Let's consider the regularity of the limit function obtained when subdividing data acquired through a point-values discretization of the function (25). In Table 1 we present numerical estimations of the regularity constant of the linear algorithm, the quasi-linear algorithm and the corrected algorithm. To obtain this table, we start from 100 initial data points and we subdivide from $L = 5$ to $L = 10$ levels of subdivision in order to obtain an approximation of the limit function. We measure the numerical regularity for $x < \frac{\pi}{6}$ assuring that the singularity is not contained in the data. From this table we can see that the numerical estimate of the regularity for the corrected algorithm is

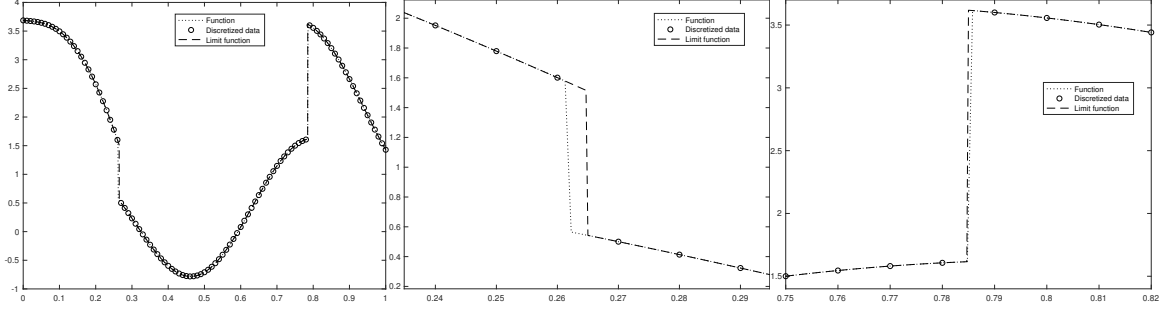


Figure 8: Limit function obtained after 5 levels of subdivision using the corrected algorithm for a piecewise continuous function. The initial data has 100 points.

very close to the one obtained by the linear scheme. The quasi-linear scheme clearly is less regular.

	L	5	6	7	8	9	10
β_1	Linear	0.8117	0.8335	0.8507	0.8647	0.8763	0.8861
	Quasi-linear	-6.0754	-0.9273	0.03565	0.0723	0.1556	0.3724
	Corrected	0.9967	0.9983	0.9992	0.9996	0.9998	0.9999
β_2	Linear	0.0167	0.0084	0.0042	0.0021	0.0011	0.0005
	Quasi-linear	-9.5160	-1.9331	-0.9654	-0.9281	-0.8446	-0.6277
	Corrected	0.5414	0.2706	0.1156	0.0491	0.0227	0.0103

Table 1: Numerical estimation of the limit functions regularity $C^{1+\beta_1-}$ and $C^{2+\beta_2-}$ for the different schemes presented and the function in (25).

5.3 Grid refinement analysis in the point-values sampling case

In this subsection we present an experiment oriented to check the order of accuracy of the schemes presented. In order to do this, we check the error of interpolation in the infinity norm obtained in the whole domain and then we perform a grid refinement analysis. We define the order of accuracy of the reconstruction as,

$$order_{k+1} = \log_2 \left(\frac{E^k}{E^{k+1}} \right),$$

E^k being the error obtained with a grid spacing h_k and E^{k+1} the error obtained with a grid spacing $h_k/2$.

We use the discrete l_∞ norm,

$$\|f^k\|_\infty = \max_{j=0,\dots,N_k} \{|f_j^k|\}.$$

Taking a fine mesh $\{x_j\}_{j=0,\dots,N_k}$, we compute

$$E_\infty^k = \|f^L - S_k^L(f^k)\|_\infty, \quad (28)$$

where f^L is the original data at the resolution L and $S_k^L(f^k)$ is the result obtained by the subdivision scheme when applied $L - k$ times to the data at the resolution k . Table 2 presents the results obtained by the three algorithms. In order to obtain this table we have applied the subdivision scheme 10 times to the original data, thus, $L - k = 10$. The data at the resolution k has been obtained through the sampling of the function in (25). We can see how the linear algorithm losses the accuracy due to the presence of the discontinuity, while the quasi-linear algorithm and the corrected approach keep high order of accuracy in the whole domain.

N_k	Corrected		Linear		Quasi-linear	
	E_∞^k	$order_k$	E_∞^k	$order_k$	E_∞^k	$order_k$
17	2.3041e-02	-	1.1052e-01	-	2.6140e-02	-
35	5.3611e-03	2.1036	4.0630e-02	1.4437	5.3611e-03	2.2856
65	1.6162e-04	5.0518	2.9258e-02	0.4737	1.6164e-04	5.0516
129	2.7694e-05	2.5450	5.2048e-03	2.4909	2.7694e-05	2.5452
257	1.7574e-06	3.9780	2.5469e-03	1.0311	1.7574e-06	3.9780
513	1.0309e-07	4.0916	1.2169e-03	1.0655	1.0309e-07	4.0916
1025	5.3956e-09	4.2559	8.9145e-04	0.4490	5.3966e-09	4.2557
2049	2.2313e-10	4.5958	7.8471e-04	0.1840	2.2408e-10	4.5899

Table 2: Grid refinement analysis in the l^∞ norm for the function in (25) for the three subdivision schemes analyzed.

It is important to remark that for any initial data obtained from a piecewise polynomial function of degree smaller or equal than three, the corrected subdivision scheme and the quasi-linear method will obtain an error equal to the machine precision.

We can also try to check the accuracy attained by the corrected subdivision scheme when working with piecewise continuous functions as the ones analyzed in Subsection 5.1. For the next experiment, the data at the resolution k has been obtained through the sampling of the function

in (25) with $a = 10$, that is a piecewise continuous function with a jump discontinuity of size a at $x = \frac{\pi}{6}$. The philosophy of this experiment is the one explained in Subsection 5.1: as the exact position of the discontinuity is lost when discretizing a function by point-values, we consider that the discontinuity is placed at the middle of the suspicious intervals. Then, in order to obtain the error and the order of accuracy, we compare with the original function but with the discontinuity placed in the middle of the suspicious interval. The results are presented in Table 3 and we can see that the corrected algorithm attains the maximum possible accuracy in the infinity norm.

N_k	Corrected	
	E_∞^k	$order_k$
17	3.6320e-02	-
35	2.5607e-03	3.8262
65	1.5596e-04	4.0373
129	9.1954e-06	4.0841
257	5.6303e-07	4.0296
513	3.4794e-08	4.0163
1025	2.1618e-09	4.0085
2049	1.3470e-10	4.0044

Table 3: Grid refinement analysis in the l^∞ norm for the corrected subdivision scheme for the function in (25), that in this case is a piecewise continuous function with a jump discontinuity in the function equal to $a = 10$. In this case, as the exact position of the discontinuity is lost when discretizing a function through the point-values, we consider that the discontinuity of the function in (25) is not placed at $\pi/6$ but at the middle of the suspicious interval.

5.4 Subdivision of bivariate point-values data

Taking into account what has been explained in previous subsections, we can try to subdivide two dimensional data. Let's consider for example the next bivariate function,

$$f(x) = \begin{cases} \cos(\pi x) \cos(\pi y), & \text{if } (x + \frac{1}{2})^2 + (y - \frac{1}{2})^2 < 1 \\ 1 - \cos(\pi x) \sin(\pi y), & \text{if } (x + \frac{1}{2})^2 + (y - \frac{1}{2})^2 \geq 1, \end{cases} \quad (29)$$

that has been represented in Figure 9. In this case we need to know the position of the discontinuity, for example through a level set function.

We can proceed as follows:

- Detect and locate the possible discontinuities using the rows and/or the columns of the data. Fit a curve or construct a level set surface that allows to locate the position of the discontinuities in the y and x direction with at least $O(h)$ accuracy.
- Obtain and store the one dimensional correction term for all the rows.
- Add the correction term to the rows and subdivide the rows using the linear algorithm.
- Subdivide the columns of the data that have been corrected in the x direction.
- Subdivide the columns of the correction term, that is a smooth function in the whole domain.
- Use the level set function to set to zero the high resolution correction term where we do not need to correct the subdivided data.
- Subtract the masked correction term from the subdivided data.

Of course, in order to apply this technique successfully, it is necessary that discontinuities are far enough from each other and from the boundaries. Figure 9 top to the left presents the original bivariate data sampled from the function in (29). Top to the right we present the resultant subdivided data obtained following the process described before. Bottom left we can observe the subdivided correction term, that is clearly smooth. Bottom to the right we can see the subdivided and masked correction term.

6 Numerical results for the case of cell-averages data

In this section we work with piecewise continuous functions supposing that the data is discretized by cell-averages, so that we are able to localize the position of the discontinuity up to the accuracy needed.

In all the experiments presented in this section we will use the following function discretized by cell-averages,

$$f(x) = \begin{cases} 10 + \left(x - \frac{\pi}{6}\right) \left(x - \frac{\pi}{6} - 10\right) + x^2 + \sin(10x), & \text{if } x < \frac{\pi}{6}, \\ x^2 + \sin(10x), & \text{if } x \geq \frac{\pi}{6}, \end{cases} \quad (30)$$

with $x \in [0, 1]$. It is easy to check that for the primitive F of f , the jump in the function at $x = \frac{\pi}{6}$ is $[F(x = \pi/6)] = 0$, the jump in the first derivative

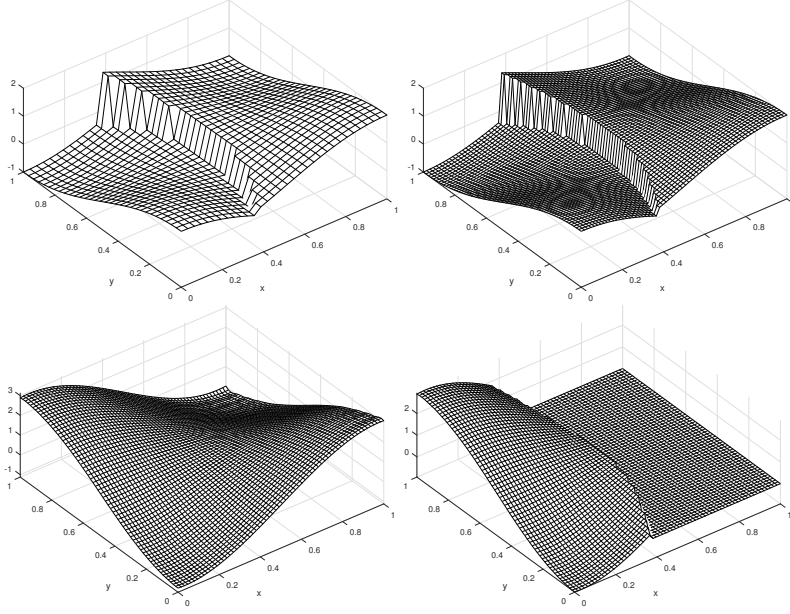


Figure 9: Top to the left, plot of the function in (29). Top to the right, subdivided data. Bottom to the left subdivided correction term. Bottom to the right masked subdivided correction term

is $[F'(x = \pi/6)] = -[f(x = \pi/6)] = -10$ and in the second derivative is $[F''(x = \pi/6)] = [f'(x = \pi/6)] = 10$.

Figure 10 shows the limit function obtained by the linear algorithm (left), the quasi-linear algorithm (center) and the corrected algorithm (right). In order to obtain these graphs we have started from 20 initial cell-averages of the function in (30). When discretizing the function in (30) through the cell-averages, we have represented the data at the lowest resolution \bar{f}_j^0 at the positions $x_{j-1}^0 + \frac{h_0}{2}$. Figure 10 shows that the linear algorithm produces oscillations close to the discontinuity. The corrected and the quasi-linear algorithms do not produce oscillations and attain a very good approximation close to the discontinuities. Figure 11 shows a zoom around the discontinuity. It is important to mention here that the point attained in the middle of the jump by the quasi-linear method and the corrected algorithm is not due to diffusion introduced by the algorithms, it is due to the kind of discretization used. Mind that, if the function presents a discontinuity in the interval (x_{j-1}^k, x_j^k) , then the discretization in (4) will always return a cell value at some point in the middle of the jump, that can be observed

in the graphs of Figures 10 and 11. This value simply corresponds to the mean of the function in the interval that contains the discontinuity, i.e. the cell-average value in (4).

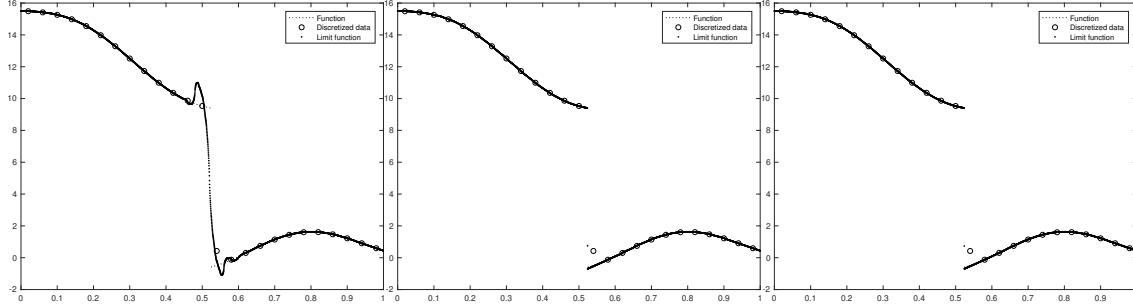


Figure 10: Limit function obtained by the linear algorithm (left), the quasi-linear algorithm (center) and the corrected algorithm (right). In order to obtain these graphs, we have started from 20 initial cell-averages of the function in (25).

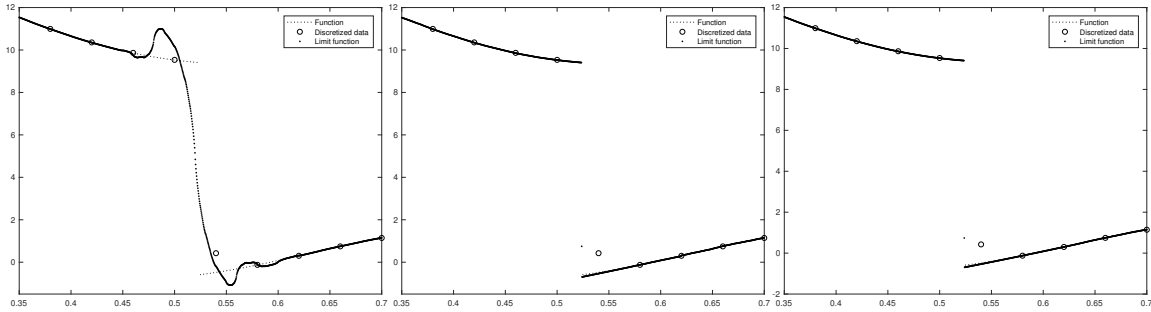


Figure 11: Zoom of the limit functions shown in Figure 10 obtained by the linear algorithm (left), the quasi-linear algorithm (center) and the corrected algorithm (right).

6.1 Numerical Regularity in the cell-average case

In this subsection we analyze the numerical regularity attained by each of the algorithms for data discretized by cell-averages. In Table 4 we present some numerical estimations of the regularity constant of the different algorithms analyzed. The data has been obtained from the discretization through cell-averages of the function in (30). Following what was done in the point-values

discretization, in order to obtain this table we start from 100 initial data cells and we subdivide from $L = 5$ to $L = 10$ levels of subdivision in order to obtain an approximation of the limit function. We measure the numerical regularity for $x < \frac{\pi}{6}$, assuring that the discontinuity is not contained in the data. From this table we can see that the numerical estimate of the regularity for the corrected algorithm is close to the one obtained by the linear scheme. The quasi-linear scheme seems to be less regular.

	L	5	6	7	8	9	10
β_1	Linear	0.2240	0.8134	0.8348	0.8518	0.8656	0.8771
	Quasi-linear	-8.1221	0.5087	-0.7584	0.1382	0.3238	-9.3917e-03
	Corrected	0.9981	0.9991	0.9995	0.9998	0.9999	0.9999
β_2	Linear	-0.7327	2.3471e-03	1.175e-03	5.8784e-04	2.9401e-04	1.4704e-04
	Quasi-linear	-12.2278	-0.4911	-1.7577	-0.8619	-0.67621	-1.0095
	Corrected	0.2886	0.1270	5.9099e-02	2.9719e-02	9.8887e-03	4.9282e-03

Table 4: Numerical estimation of the limit functions regularity C^{β_1-} and $C^{1+\beta_2-}$ for the different schemes presented and the function in (30) discretized by cell-averages.

6.2 Grid refinement analysis for the cell-averages sampling

In this section we reproduce the grid refinement analysis that we performed for the point-values' case, using the infinity norm in (28), but we also use the l^1 norm. Taking the mesh $\{x_j^k\}_{j=0,\dots,N_k}$, we compute

$$E_1^k = h_k \sum_{j=1}^{N_k} |\bar{f}_j^k - S(\bar{f}^{k-1})_j|,$$

where, now $\bar{f}_j^k = \frac{1}{h_k} \int_{x_{j-1}^k}^{x_j^k} f(x) dx$ is a cell-average value of the function at the resolution k , (4). In this case $S(\bar{f}^{k-1})_j$ is the result obtained by the subdivision scheme applied to the point-values of the primitive (5) of \bar{f}^{k-1} and then returned to the cell-average values at the level k using (6). N_k is the length of \bar{f}^k and $S(\bar{f}^{k-1})_j$ at the resolution k .

In this case we have used the function presented in (30) discretized by cell-averages. Table 5 presents the errors and orders of approximation obtained by the three algorithms in the infinity norm. For our approach we show the error outside the interval $[x^*, s^*]$, in order to check the results stablished in Theorem 3.5. For the linear and quasi-linear subdivision schemes

we present the infinity norm in the whole domain. We can see how the linear algorithm losses the accuracy close to the discontinuity, while the quasi-linear algorithm and the corrected approach keep high order of accuracy. In particular, the corrected algorithm attains $O(h^3)$ accuracy, that is in accordance with the results of Theorem 3.5. We can also perform the same grid refinement analysis but using the l^1 norm instead. The results are presented in Table 6. We can see in this table that we attain the order of accuracy expected. Mind that the accuracy has been reduced by one for all the algorithms as we are using a subdivision algorithm with a stencil of three cells. The corrected approach attaches the same order of accuracy as the quasi-linear algorithm.

	Corrected		Linear		Quasi-linear	
N_k	E_∞^k	$order_k$	E_∞^k	$order_k$	E_∞^k	$order_k$
64	1.2739e-02	-	5.1079	0.3483	6.0545e-01	2.3782
128	2.3556e-03	2.4350	5.5371	-0.1164	2.9149e-01	1.0546
256	5.9829e-04	1.9772	5.8782	-0.0862	3.1212e-02	3.2232
5012	6.5693e-05	3.1870	6.2890	-0.0975	3.2997e-03	3.2417
1024	7.3102e-06	3.1678	6.5697	-0.0630	3.1356e-04	3.3955
2048	7.8325e-07	3.3820	6.0839	0.1108	1.7553e-05	4.1589

Table 5: Grid refinement analysis after ten levels of subdivision in the l^∞ norm for the function in (30) discretized by cell-averages and for the three subdivision schemes presented.

	Corrected		Linear		Quasi-linear	
N_k	E_1^k	$order_k$	E_1^k	$order_k$	E_1^k	$order_k$
64	1.2052e-03	-	1.2716e-01	-	2.0014e-03	-
128	1.4370e-04	3.0681	8.0777e-02	0.6546	2.7861e-04	2.8447
256	1.9401e-05	2.8889	2.2254e-02	1.8599	3.8808e-05	2.8438
512	2.0882e-06	3.2158	1.0952e-02	1.0229	4.7043e-06	3.0443
1024	2.4270e-07	3.1050	5.5043e-03	0.9925	5.8186e-07	3.0152
2048	2.9298e-08	3.0503	3.1853e-03	0.7891	7.2468e-08	3.0053

Table 6: Grid refinement analysis in the l^1 norm for the function in (30) discretized by cell-averages and for the three subdivision schemes presented.

6.3 Subdivision of bivariate cell-averages' data

In this case we have applied the algorithms analyzed in previous sections to two-dimensional data using a tensor product approach, i.e. we directly

process one-dimensional data by rows and then by columns.

In this section we will work with the bivariate function discretized by cell-averages,

$$f(x) = \begin{cases} \cos(\pi x) \cos(\pi y), & \text{if } 0 \leq x < 0.5, 0 \leq y < 0.5, \\ -\cos(\pi x) \cos(\pi y) + 2, & \text{if } 0.5 < x \leq 1, 0 \leq y < 0.5, \\ -\cos(\pi x) \cos(\pi y) + 2, & \text{if } 0 < x \leq 0.5, 0.5 \leq y < 1, \\ -\cos(\pi x) \cos(\pi y) + 4, & \text{if } 0.5 < x \leq 1, 0.5 \leq y < 1. \end{cases} \quad (31)$$

Figure 12 shows the result of one step of subdivision using the tensor product approach for the data presented in Figure 12 top to the left. This means that we apply the one dimensional subdivision scheme by rows and then by columns. The result presented in Figure 12 top to the right corresponds to the linear algorithm. We can observe that the effect of the discontinuity appears in the subdivided data in the form of diffusion and Gibbs effect. The result of the quasi-linear algorithm and the corrected approach is presented in Figure 12 bottom to the left and to the right respectively. We can see that both results are very similar. As shown in previous sections, the main difference is the regularity of the data close to the discontinuity, that is higher for the corrected approach. In terms of accuracy, both algorithms perform similar.

7 Conclusions

In this paper we have introduced a corrected implementation of a linear subdivision scheme in order to adapt the procedure for the approximation of non-smooth data. The first advantage of this approach is that the resultant scheme presents the same regularity as the linear scheme. Moreover, the theoretical analysis of the convergence and regularity is derived directly from the properties of the linear scheme. The accuracy of the corrected approach is obtained from the accuracy reached in the location of the discontinuities and in the accuracy of the approximation of the jump in the function and its derivatives, that is done through Taylor's expansions. Thus, the corrected algorithm presents the same regularity, at each regularity zone, as the linear scheme [14, 17, 18] plus the same accuracy as the quasi-linear scheme [9]. We present the results for the 4-point linear subdivision scheme, but the approach is indeed applicable to any other subdivision scheme aimed to deal with the approximation of functions with singularities. By construction, the corrected subdivision algorithm does not present Gibbs phenomenon and does not introduce diffusion. As far as we know, this is the first time that

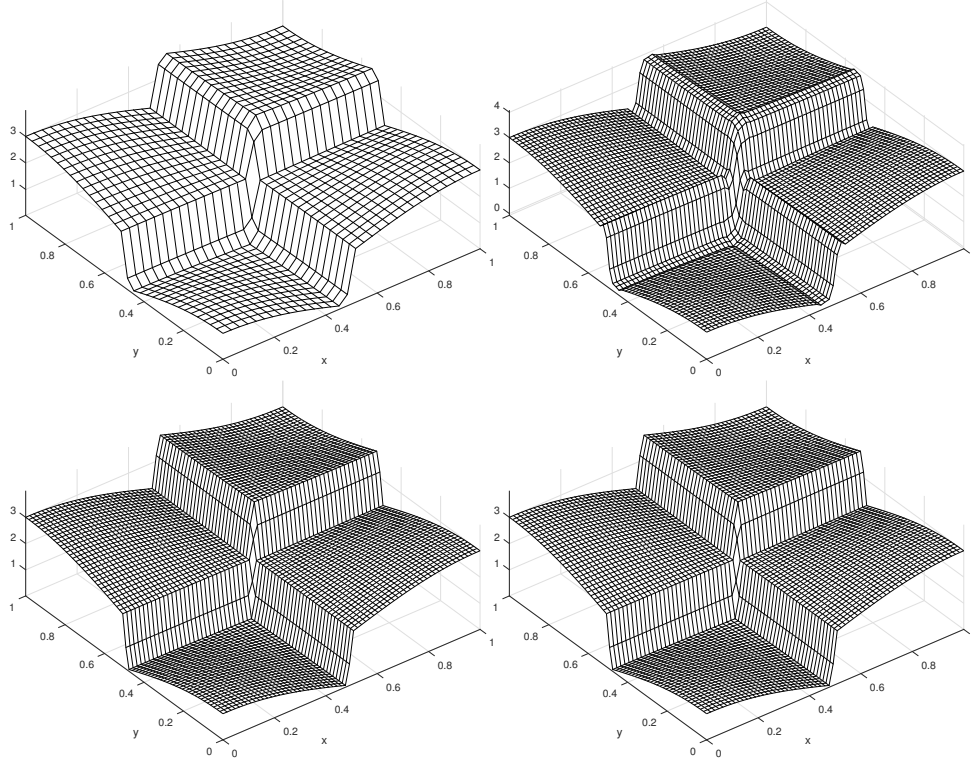


Figure 12: Result of one step of subdivision using the tensor product approach for the data presented at the top to the left. The figure at the top to the right corresponds to the linear algorithm. The result of the quasi-linear algorithm and the corrected approach is presented at the bottom to the left and to the right respectively.

subdivision schemes that own all these properties at the same time appear in the literature. The numerical results confirm our theoretical analysis.

References

- [1] Amat, S.; Li, Z.; Ruiz, J. On an new algorithm for function approximation with full accuracy in the presence of discontinuities based on the immersed interface method. *J. Sci. Comput.* 75 (2018), no. 3, 1500-1534.
- [2] Amat, S.; Liandrat, J. On the stability of PPH nonlinear multiresolution. *Appl. Comput. Harmon. Anal.* 18 (2005), no. 2, 198-206.

- [3] Amat, S.; Liandrat, J.; Ruiz, J.; Trillo, J. C. On a power WENO scheme with improved accuracy near discontinuities. *SIAM J. Sci. Comput.* 39 (2017), no. 6, 2472-2507.
- [4] Amat, S.; Ruiz, J.; Trillo, J. C. On an algorithm to adapt spline approximations to the presence of discontinuities. *Numer. Algorithms* 80 (2019), no. 3, 903-936.
- [5] Amat, S.; Dadourian, K.; Liandrat, J. On a nonlinear 4-point ternary and interpolatory multiresolution scheme eliminating the Gibbs phenomenon. *Int. J. Numer. Anal. Model.* 7 (2), (2010) 261–280.
- [6] Amat, S.; Liandrat, J. On the stability of the PPH nonlinear multiresolution, *Appl. Comp. Harm. Anal.*, 18 (2), (2005) 198–206.
- [7] Amat, S.; Ruiz, J.; Trillo, J. C.; Yáñez, D. F. Analysis of the Gibbs phenomenon in stationary subdivision schemes. *Appl. Math. Lett.*, 76, (2018) 157–163.
- [8] Amir, A.; Levin, D. High order approximation to non-smooth multivariate functions. *Comput. Aided Geom. Design* 63 (2018), 31-65.
- [9] Aràndiga, F.; Cohen, A.; Donat, R.; Dyn, N. Interpolation and approximation of piecewise smooth functions. *SIAM J. Numer. Anal.* 43 (2005), no. 1, 41-57.
- [10] Aràndiga, F.; Donat, R.; Mulet, P. Adaptive interpolation of images, *Signal Process.* (83) (2003), no. 2, 459–464.
- [11] Baccou, J.; Liandrat, J. Position-dependent Lagrange interpolating multiresolutions. *International Journal of Wavelets, Multiresolution and Information Processing* 5 (2007) no. 4, 513-539.
- [12] Beccari, C.; Casciola, G.; Romani, L. An interpolating 4-point C^2 ternary non-stationary subdivision scheme with tension control. *Comput. Aided Geom. Design*, 24 (4) (2007) 210–219.
- [13] Cohen, A.; Dyn, N.; Matei B. Quasilinear subdivision schemes with applications to ENO interpolation. *Applied and Computational Harmonic Analysis* 15 (2003) no. 2, 89-116.
- [14] Daubechies, I.; Lagarias, J. Two scale differences equations: I. Existence and global regularity of solutions, *SIAM J. Math. Anal.* 22 (1991) 1388-1410.

- [15] Deslauriers, G.; Dubuc, S. Symmetric iterative interpolation processes. *Constr. Approx* 5 (1989), 49-68 .
- [16] Dyn, N.; Levin, D. Subdivision Schemes in Geometric Modelling. *Act. Num.* 11, (2002) 73–144.
- [17] Dyn, N.; Levin, D.; Gregory, J. A. A 4-point interpolatory subdivision scheme for curve design. *Comput. Aided Geom. Design*, (4) (1987), no. 4, 257-268.
- [18] Dyn, N.; Gregory, J.; Levin, D. Analysis of uniform binary subdivision schemes for curve design, *Constr. Approx.* 7 (1991)127-147.
- [19] Hassan, M.F.; Ivriissimtzis, I.P.; Dodgson, N.A. Sabin, M.A.; An interpolating 4-point ternary stationary subdivision scheme, *Comput. Aided Geom. Design*, 19, (2002) 1–18.
- [20] Hassan, M.F.; Dodgson, N.A. Ternary and three-point univariate subdivision schemes, in: A. Cohen, J.-L. Merrien, L.L. Schumaker (Eds.), *Curve and Surface Fitting: Sant-Malo 2002*, Nashboro Press, Brentwood, (2003) 199–208.
- [21] Jeon, M.; Han, D.; Park, K.; Choi, G. Ternary univariate curvature-preserving subdivision. *J. Appl. Math. Comput.*, 18 (1-2), (2005) 235–246.
- [22] Kagan, Yael; Levin, D. High order reconstruction from cross-sections. *Curves and surfaces*, 289-303, *Lecture Notes in Comput. Sci.*, 9213, Springer, Cham, 2015.
- [23] Kuijt, F. Convexity Preserving Interpolation: Nonlinear Subdivision and Splines. PhD thesis, University of Twente, (1998).
- [24] Kwan, P.K.; Byung-Gook, L.; Gang, J.Y. A ternary 4-point approximating subdivision scheme. *App. Math. Comp.* 190, (2007) 1563–1573.
- [25] Lipman, Y.; Levin, D. Approximating piecewise-smooth functions. *IMA J. Numer. Anal.* 30 (2010), no. 4, 1159-1183.
- [26] Levin, D. Between moving least-squares and moving least- l_1 . *BIT* 55 (2015), no. 3, 781-796.
- [27] Floater, M.S.; Michelli, C.A. Nonlinear stationary subdivision, *Approximation theory: in memory of A.K. Varna*, edt: Govil N.K, Mohapatra N., Nashed Z., Sharma A., Szabados J., (1998) 209–224

- [28] Guessab, A.; Moncayo, M.; Schmeisser, G. A class of nonlinear four-point subdivision schemes. *Adv. Comput. Math.* 37(2), (2012) 151–190.
- [29] Harizanov, S.; Oswald, P. Stability of nonlinear subdivision and multi-scale transforms, *Constr. Approx.* 31(3), (2010) 359–393.
- [30] Oswald, P., Smoothness of Nonlinear Median-Interpolation Subdivision, *Adv. Comput. Math.*, 20(4), (2004) 401–423.
- [31] Qu, R. A new approach to numerical differentiation and integration. *Math. Comput. Model.* 24.10 (1996): 55-68.
- [32] Siddiqi, S.; Younis, M. Construction of m-point binary approximating subdivision scheme, *Appl. Math. Lett.* 26, (2013) 337–343.
- [33] Sharon, N.; Dyn, N. Bivariate interpolation based on univariate subdivision schemes, *J. Approx. Theory*, 164, (2012) 709–730.
- [34] Wang, H.; Qin, K. Improved ternary subdivision interpolation scheme. *Tsinghua Sci. Technol.*, 10 (1), (2005) 128–132.
- [35] Zheng, H.; Zhenglin, Y.; Zuoping, C.; Hongxing Z.; A controllable ternary interpolatory subdivision scheme. *Int. J. CAD/CAM*, 5, (2005) paper number 9.